

Video Article

Multimodal Volumetric Retinal Imaging by Oblique Scanning Laser Ophthalmoscopy (oSLO) and Optical Coherence Tomography (OCT)

Weiye Song^{*1}, Libo Zhou^{*1}, Ji Yi^{1,2}

¹Department of Medicine, Boston University School of Medicine

²Department of Biomedical Engineering, Boston University

*These authors contributed equally

Correspondence to: Ji Yi at jiyi@bu.edu

URL: <https://www.jove.com/video/57814>

DOI: [doi:10.3791/57814](https://doi.org/10.3791/57814)

Keywords: Retraction, Issue 138, Oblique scanning laser ophthalmoscopy, multimodal, volumetric retinal imaging

Date Published: 8/4/2018

Citation: Song, W., Zhou, L., Yi, J. Multimodal Volumetric Retinal Imaging by Oblique Scanning Laser Ophthalmoscopy (oSLO) and Optical Coherence Tomography (OCT). *J. Vis. Exp.* (138), e57814, doi:10.3791/57814 (2018).

Abstract

While fluorescence imaging is widely used in ophthalmology, a large field of view (FOV) three-dimensional (3D) fluorescence retinal image is still a big challenge with the state-of-the-art retinal imaging modalities because they would require z-stacking to compile a volumetric dataset. Newer optical coherence tomography (OCT) and OCT angiography (OCTA) systems overcome these restrictions to provide three-dimensional (3D) anatomical and vascular images, but the dye-free nature of OCT cannot visualize leakage indicative of vascular dysfunction. This protocol describes a novel oblique scanning laser ophthalmoscopy (oSLO) technique that provides 3D volumetric fluorescence retinal imaging. The setup of the imaging system generates the oblique scanning by a dove tail slider and aligns the final imaging system at an angle to detect fluorescent cross-sectional images. The system uses the laser scanning method, and therefore, allows an easy incorporation of OCT as a complementary volumetric structural imaging modality. *In vivo* imaging on rat retina is demonstrated here. Fluorescein solution is intravenously injected to produce volumetric fluorescein angiography (vFA).

Video Link

The video component of this article can be found at <https://www.jove.com/video/57814/>

Introduction

Ophthalmology and vision science greatly benefit from the modern optical imaging techniques, since the retina can be easily accessed with light. Fluorescence retinal imaging is an essential tool in the diagnosis and management of chorioretinal vascular diseases such as diabetic retinopathy (DR) and age-related macular degeneration (AMD), both of which are leading causes of blindness in the United States.

However, it is still challenging to acquire a large field of view (FOV), three-dimensional (3D) retinal imaging by using fluorescence imaging. Fundus photography does not have the depth-resolving capability and does not reject diffuse light. As a result, the mixing of signals from different depth reduces the image quality. Scanning laser ophthalmoscopy (SLO) and confocal SLO (cSLO) can reduce the effect of diffused light by using confocal gating¹. However, it is difficult for SLO or cSLO to acquire a 3D human retinal image due to the limit of their depth of focus. Adaptive optics SLO (AOSLO) can provide superb resolution and contrast by correcting for the wavefront aberrations introduced by the human eye. However, AOSLO would still need z-stacking for volumetric imaging². Optical coherence tomography (OCT)³ and OCT angiography (OCTA) systems overcome these restrictions to provide three-dimensional (3D) anatomical and vascular images^{4,5,6}, but the dye-free nature of OCT cannot visualize leakage indicative of vascular dysfunction.

This protocol describes a novel multimodal platform for 3D volumetric fluorescence retinal imaging, namely oblique scanning laser ophthalmoscopy (oSLO). In this imaging system, an oblique scanning is generated by a dove tail slider, and a final imaging system is aligned in an angle to detect fluorescence cross sectional images. The system uses laser scanning methods, and these techniques allow easy incorporation with OCT as a complementary volumetric structural imaging modality. The current depth resolution is about 25 μm in the rat retina and the field of view is 30°. Essentially, the oSLO allows a fluorescent version of OCT and can be simultaneously combined with OCT and OCTA over a large FOV.

In this protocol, we will describe the setup of the oSLO, the method of alignment and construction, the method of *in vivo* imaging of rat retina, and the representative results.

Protocol

All methods described here have been approved by the Animal Care and Use Committee (ACUC) of Boston Medical Center.

1. System Setup

1. oSLO System

1. Use a supercontinuum laser source as the system laser source.
 1. Separate the visible light range (450-650 nm) from higher wavelength range (650-2000 nm) by a dichroic mirror (DM1). Expand the spectrum with a pair of dispersive prisms after the beam passing through a polarization beam splitter (PBS).
 2. Place a slit to select the excitation wavelength range (475-495 nm). Use a reflective mirror to reflect the filtered beam back to the prism pair and then couple the light into a single mode fiber (SMF 1).
 3. Use a spectrometer to confirm the wavelength selection at the output of the single mode fiber.
2. Connect the single mode fiber to two cascaded optical fiber couplers as shown in **Figure 2**. One of the fiber output port from the second fiber coupler delivers the light to the oSLO system.
3. Collimate the laser first in the oSLO system.
 1. Deflect the laser by a galvanometer mirror (GM1). Relay the laser to a second galvanometer mirror (GM2) by a 1:1 telescope system, and further relay to the pupil of the eye by a 3:1 telescope system.
 2. Install a dichroic mirror (DM2) within the 3:1 telescope system to reflect the fluorescence signals.
4. Mount the 3:1 telescope system and the dichroic mirror (DM2) on a customized dove tail slider to offset the optical axis and create the oblique scanning illumination as shown in **Figure 3**. Use a caliper to precisely control the offset length as desired.
5. Fluorescence imaging optical path.
 1. Reflect the fluorescence by the dichroic mirror and relay to the third galvanometer mirror to de-scan the slow scanning.
 2. Relay the light to an imaging objective lens by another 1:1 telescope system. Install the above optics on a translation stage. NOTE: Two additional translation stages are installed under the third galvanometer mirror (GM3) to provide redundancy in the degrees of freedom for optimizing the imaging.
6. Mount a final imaging system on a stage that has three degrees of freedom (rotation, and two axis of translation). Use a planar camera to capture the cross-sectional fluorescence images.

2. Optical Coherence Tomography System

1. Use the same supercontinuum laser source as the system laser source.
 1. Separate the near infrared (NIR) range (650-900 nm) from the remaining light (650-2000 nm) by another dichroic mirror (DM3). Use a long pass filter to further limit the bandwidth to 800-900 nm. Couple the beam into a single mode fiber (SMF 2).
2. Connect the single mode fiber to the other input port of the two cascaded optical fiber couplers to combine with the blue oSLO excitation. Direct the light from the second output port of the second fiber coupler to the OCT reference arm, which has a variable neutral density filter (VNDF), dispersion compensation plates and a reflective mirror. NOTE: The light returned from the reference arm and the eye recombines at the second optical fiber coupler and is delivered to the OCT spectrometer to collect the signal.

3. Data Acquisition

1. Use a data acquisition system software written in LabVIEW and modified from the scanning protocol of OCTA^{7,8,9,10}. For each B-scan, an 80% duty cycle saw tooth with 500 steps is output by an analog output board (AO1) to control the x' fast scanning mirror, GM2.
2. Trigger the line scan camera at each step to acquire data for the OCT only when the mirror is in the forward scanning direction. Set the exposure time for the line scan camera to be 17 μ s.
3. To acquire the OCTA signal, repeat the measurement 5 times at the same B-scan location.
4. Set the AO output rate at 100 kHz, and the OCT A-line rate at 50 kHz. Control the y' slow scanning mirror, GM1, by a ramping waveform. Synchronize the de-scanning mirror, GM3, with GM1 to de-scan the slow scanning.
5. Trigger the planar camera by another analog output board (AO2) to capture one fluorescent image at each y' location. Crop the imaging size or bin the neighbor pixels to increase the speed and sensitivity as desired.

2. System Alignment

1. Adjust the slit in the oSLO light source to select the blue excitation wavelength. Use a spectrometer to monitor the spectral range to be around 475-490 nm.
2. Adjust the dove tail mount slider to shift the optical axis by ~5 mm. This will result in an offset at the rat pupil by ~1.7 mm, resulting in an oblique angle of ~15° on the retina.
3. Adjust the translation stage of the fluorescence detection optics by the same 5 mm.
4. Adjust the final fluorescence imaging system to be ~30°.
5. Measure the optical power using a power meter. Make sure the blue oSLO excitation power is ≤ 0.2 mW and the OCT laser power ≤ 0.8 mW, which will not cause retina damage. NOTE: Based on the ANSI standard, the maximum permissive exposure (MPE) to the retina is at the level of $\sim 2 \text{ mW}^{7,8}$ in visible light range. According to the formula by Delori *et al.*⁹, the MPE for the near infrared light is about two times higher than the visible light, at about 4 mW.

3. In Vivo Animal Experiment

1. Transfer a 12-weeks male Long Evans rat into the induction chamber. Anesthetize the rat with 4.5% isoflurane in oxygen for 10 minutes with a flow rate of 2 L/min by an isoflurane vaporizer.

1. Confirm depth of anesthesia as determined by a lack of withdrawal reflex during an interdigital pinch.
2. After the induction, place the rat on a 5-axis (x, y, z translations, yaw and pitch) holder. Provide supplemental heat by use of a heated stage, circulating warm water blanket or other suitable method in a prolonged experiment. Maintain the anesthesia at 1.5% of isoflurane with a flow rate of 2 liter/minutes during the remaining part of the experiment. When not using an induction chamber with active exhaust, the induction chamber should be placed on a backdraft or downdraft table or under a snorkel to scavenge isoflurane.
3. Dilate the pupil with 1% Tropicamide ophthalmic solution for 2 minutes. Apply 0.5% Tetracaine HCl ophthalmic solution on the rat's eye for additional local anesthesia, if necessary. Keep the eye moisturized with commercial artificial tears at least once every minute during the experiment.
4. Inject fluorescein salt (10% w/w) or FITC (10% w/w) diluted in sterile saline (0.1-0.3 mL) through the tail vein with a 1 mL syringe and a 29G needle.
5. Turn on the laser source. Place a neutral density filter to attenuate the blue light excitation during alignment. Measure the power of the OCT light to be ~0.8 mW, and the blue light <0.01 mW to avoid the formation of cataracts.
6. Start the galvanometer scanning and alignment mode. Adjust the height of the eye ball to make a stationary laser spot on the cornea. Adjust the rat eye position to make the rim of the pupil roughly perpendicular to the laser, and offset the laser to the apical center of the eye to about ~1.5 mm.
7. Further adjust the animal holder until OCT images reach optimal quality. In the x' fast scanning direction, make sure that the cross-sectional B-scan image appears flat. When switching to the y' slow scanning direction, make sure the cross-section B-scan image appears tilted, due to the oblique scanning.
8. Remove the neutral density filter to the blue light excitation and monitor the real time feed from the camera. Cross sectional fluorescent image should appear showing blood vessels appearing in different depths.
 1. Adjust the focus of the final fluorescence imaging system to reach the optimal focus. Allow fine adjustments of the eye position in the lateral plane to reach optimal oSLO image quality.
9. After the alignment, start to acquire simultaneous OCTA and volumetric fluorescein angiography (vFA).
10. Construct the volumetric images for both OCTA and oSLO by Matlab. The algorithms are previously described in detail¹⁰. Generate depth-resolved retinal vasculatures by image segmentation.
11. After completing the imaging, turn off the laser, release the animal and apply some ophthalmic ointment on the eyes, and then place the animal in a recovery box.
12. Do not leave the animal unattended until it has regained sufficient consciousness to maintain sternal recumbency or as per institutional policy.

Representative Results

Figure 4a shows a cross-sectional OCT image of a rat retina. **Figure 4b-4c** show the same retinal cross-sectional images of OCTA and oSLO vFA acquired at the same time. The oSLO enables cross-sectional FA analogous to the OCT B-scan. In comparison to OCTA, the oSLO vFA cross-sectional image clearly identifies the vessels in nerve fiber layer (NFL) and ganglion cell layer (GCL), and capillaries in outer plexiform layer (OPL). **Figure 4d** and **4g** show the superficial layer of OCTA and oSLO vFA image. Unlike OCTA, the oSLO vFA image (**Figure 4g**) avoids the motion artifacts (vertical stripes in **Figure 4d**) by utilizing fluorescence emission contrast. By comparing the oSLO vFA (**Figure 4e**) and OCTA (**Figure 4h**) images within the retinal intermediate layer, the vertically diving vessels are clearly shown in the oSLO FA image but not apparent in OCTA. This is presumably because the blood flow speed or the vessel orientation will affect the OCTA signal but not the oSLO fluorescence contrast.

Figure 4f and **4i** show the images within the deep capillary plexus layer. The regions pointed out by blue arrows in oSLO vFA have a better contrast than OCTA in the vasculature. The size of the venule pointed out by white arrows in oSLO is larger than that in OCTA. Overall, the oSLO vFA image resembles the actual vascular morphology more accurately than OCTA, since it is not dependent upon blood flow speed or the vessel orientation. An *en face* fly-through from two simultaneously acquired volumetric data set from oSLO and OCTA are shown in **Video 1**.

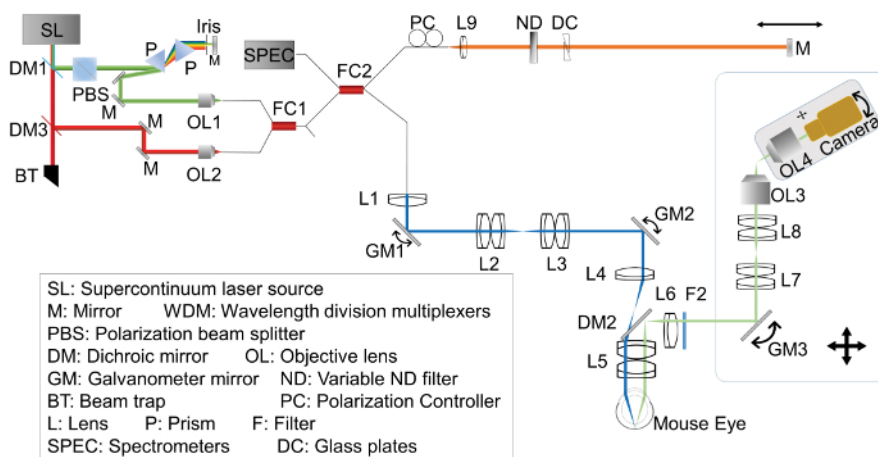


Figure 1. The system schematic. Please click here to view a larger version of this figure.

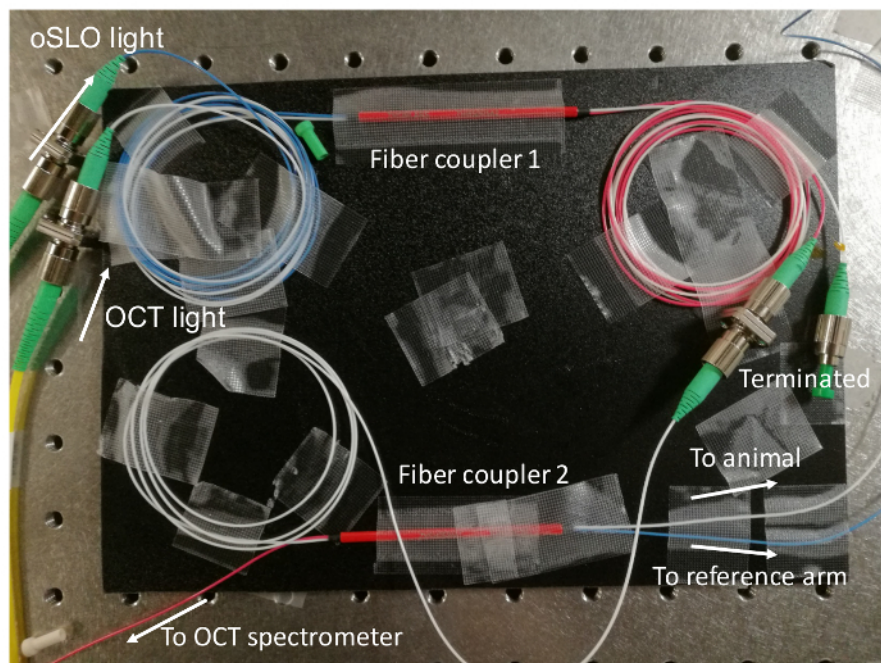


Figure 2. The photograph of the two cascaded fiber couplers that direct oSLO and OCT light. The routes of the light pass are labeled. [Please click here to view a larger version of this figure.](#)

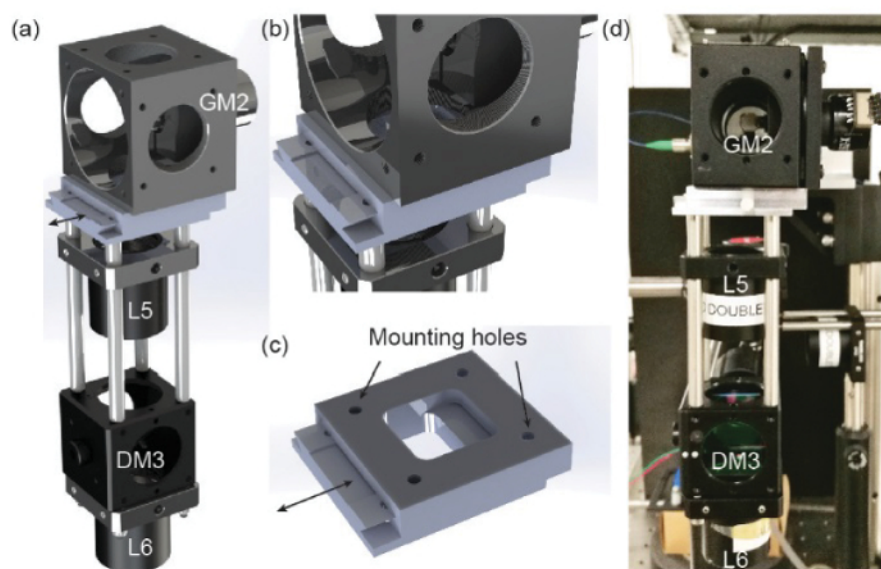


Figure 3. The setup of the dove tail mount for oblique illumination. (a) The solid work model for the oblique illumination part. (b-c) The zoomed-in view, and the separate view of the dove tail mount. (d) The photograph of the actual setup for oblique illumination part. [Please click here to view a larger version of this figure.](#)

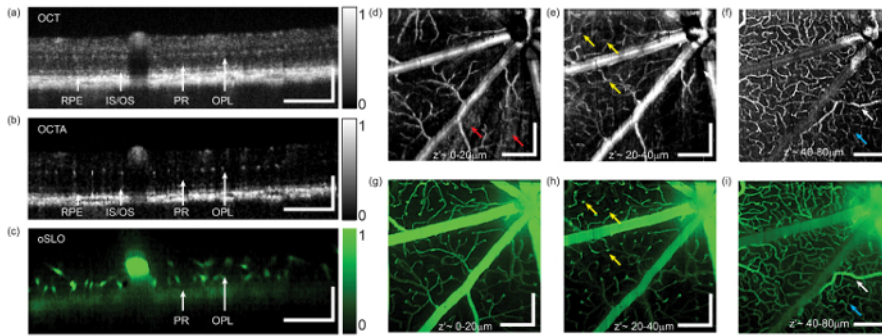


Figure 4. Rat retinal image acquired by oSLO and OCTA at the same time. The example of (a) the cross-sectional image of OCT (b) OCTA and (c) oSLO FA. Panels (d) and (g) show *en face* OCT and oSLO FA images from the superficial layer. The motion artifacts in OCTA image was pointed out by red arrows. Panel (e) and (h) show the results from the intermediate layer. The locations where the vessels dive down into next layer were pointed out by yellow arrows, which are clearer on oSLO FA than OCTA. Panels (f) and (i) show the results from the deep capillary plexuses layer. The contrast of oSLO is better than OCTA in the region pointed out by blue arrows. The size of the venule pointed out by white arrows in oSLO is larger than that in OCTA. Bars in the figure is 200 μm . [Please click here to view a larger version of this figure.](#)

Discussion

Here, we have described oSLO, an *in vivo* volumetric fluorescent retinal imaging technique with a FOV over 30° . Compared to OCT, a current standard of care imaging method in ophthalmology, oSLO offers a similar 3D imaging capability yet allows fluorescence contrast that OCT is not sensitive to. The advantage of oSLO is that it requires only one raster scan, and thus allows the seamless combination of OCT, providing two complementary techniques for structural and fluorescent volumetric imaging.

In this protocol, the key point to obtain good image quality is the clarity of the rat eye. If the oSLO image is obscured, examine whether there is cataract formation. Several factors such as ketamine/xylazine anesthesia, cornea drying, and over-exposure to blue light will cause formation of cataracts, which would significantly deteriorate the image quality. To prevent the cataracts, avoid continuous exposure to blue light for more than 2 minutes; apply artificial eye tear at least once every minute to prevent cornea drying; and allow the eye to rest at least 30 seconds between imaging sections by blocking the light.

We envision that oSLO can significantly impact the clinical practice of fluorescence imaging. We have shown that the depth resolving power can effectively eliminate the signal from the outer retinal, yielding high-contrast volumetric FA images down to the single capillary level, which is unobtainable with conventional SLO. The dramatically improved image clarity would allow for more sensitive detection and quantification of blood-retina barrier disruption and retinal capillary leakage, the hallmark of vision-threatening macular edema in DR and other chorioretinal vascular diseases.

In the current system, the speed of the CCD camera is 20 frames per second, which leads to >25 second acquisition times. A scientific CMOS camera will dramatically improve the system speed. The fluorescence detection has a different optical path separated from the illumination. It will simplify the system if using the same optical path for the illumination and detection in the future design. In summary, a novel multimodal platform for volumetric retinal imaging, namely oblique scanning laser ophthalmoscopy (oSLO), was presented. The large FOV *in vivo* imaging over a 30° viewing angle of rat retina using oSLO and simultaneous optical coherence tomography (OCT) was demonstrated.

Disclosures

Ji Yi holds a pending patent for oSLO. The other author(s) declare no competing financial interests.

Acknowledgements

Funding is from the Evans Medical foundation funding from Boston Medical Center as well as a sub-contract from NIH 5R01CA183101, BU-CTSI pilot grant 1UL1TR001430, BU-Joslin pilot program, and BU-CTSI KL2TR001411.

References

- Webb, R. H., Hughes, G. W., & Delori, F. C. Confocal scanning laser ophthalmoscope. *Applied Optics*. **26** (8), 1492-1499 (1987).
- Roorda, A. *et al.* Adaptive optics scanning laser ophthalmoscopy. *Optics Express*. **10** (9), 405-412 (2002).
- Huang, D. *et al.* Optical coherence tomography. *Science*. **254** (5035), 1178-1181 (1991).
- de Carlo, T. E., Romano, A., Waheed, N. K., & Duker, J. S. A review of optical coherence tomography angiography (OCTA). *International Journal of Retina and Vitreous*. **1** (1), 5 (2015).
- Jia, Y. *et al.* Quantitative Optical Coherence Tomography Angiography of Choroidal Neovascularization in Age-Related Macular Degeneration. *Ophthalmology*. **121** (7), 1435-1444 (2014).
- Chen, C.-L., & Wang, R. K. Optical coherence tomography based angiography [Invited]. *Biomedical Optics Express*. **8** (2), 1056-1082 (2017).
- Yi, J., Chen, S. Y., Shu, X., Fawzi, A. A., & Zhang, H. F. Human retinal imaging using visible-light optical coherence tomography guided by scanning laser ophthalmoscopy. *Biomedical Optics Express*. **6** (10), 3701-3713 (2015).

8. Zhang, X. Y. *et al.* Dual-band spectral-domain optical coherence tomography for *in vivo* imaging the spectral contrasts of the retinal nerve fiber layer. *Optics Express*. **19** (20), 19653-19667 (2011).
9. Delori, F. C., Webb, R. H., & Sliney, D. H. Maximum permissible exposures for ocular safety (ANSI 2000), with emphasis on ophthalmic devices. *Journal of the Optical Society of America a-Optics Image Science and Vision*. **24** (5), 1250-1265 (2007).
10. Zhang, L. *et al.* Volumetric fluorescence retinal imaging *in vivo* over a 30-degree field of view by oblique scanning laser ophthalmoscopy (oSLO). *Biomedical Optics Express*. **9** (1), 25-40 (2018).